Effect of Antisolvents Treatment on the Performance of Monolithic Perovskite Solar Cells

Bhagavan Reddy Thokala[1, a], D.N. Prasad[2,b*] and Kumar Manoj[1,c]

[1]Department of Electronics & Communications Engineering (ECE), Himalayan University, Itanagar, Arunachal Pradesh, 791111, India.

[2]Department of Humanities & Sciences, VNR Vignana Jyothi Institute of Engineering and Technology, Vignana Jyothi Nagar, Bachupally, Nizampet,

Hyderabad, Telangana, 500090, India.

[a]bhagavanreddythokala@gmail.com , [b]nagendraprasad_d@vnrvjiet.in, [c]drmanoj@mits.ac.in*

Abstract:

Currently Anti-solvent treatment (A.S.T) has emerged as one of the key techniques for creating highly efficient monolithic perovskite solar cells (mPSCs). Perovskite film quality issues, such as uneven surfaces and pinholes, are present in perovskite solar cells and have a direct impact on device performance. To enhance the perovskite film quality and device performance introduced ant solvent treatment method. It has been observed that the AST technique improved the solar cell efficiency, reduced hysteresis and stability. It has become achievable to produce uniform and pinhole free perovskite film with the AST that enhances the nucleus density during film formation. In the current research, MScs were fabricated by different anti-solvents such as, Diethyl ether (DE), Chloroform (CF), O-Dichloride benzene (ODB), Chlorobenzene (CB), and Toluene (T). X-Ray Diffraction (XRD) and Scanning electron microscopy (SEM) were employed to evaluate the fabricated MScs. The power conversion efficiency (PCE) of perovskite through Toluene ant solvent results shows 4.21% as compared with pure perovskite (PCE; 3.93%) and other (DE, CF, ODB, CB) anti-solvents.

Keywords: Monolithic perovskite solar cells, Anti-solvent treatment, Pinhole free-homogeneous film, Power conversion efficiency.

1. Introduction

Nowadays, researchers are attentive toward perovskite solar cells (PSCs) because of their ability in increasing PCE, and cost-effectiveness in fabrication [1, 2]. The monolithic carbon electrodes are found to be a promising candidate in this scenario with their exceptional electrical conductivity and high stability [3, 4]. The deposition process such as drop-casting, inkjet-printing, press transferring, rolling transfer, doctor-blading, and screen printing are adapted on carbon electrodes [5, 6]. The problems faced while commercializing these solar cells are reliability and stability [7–10]. Stability can be enhanced either by encapsulation technologies or by additive engineering methods, but still not suitable for commercialization [11–14].

The challenge faced while fabrication was unique perovskite film formation without pinhole to achieve higher efficiency. Because pinholes decrease shunt resistance and non-uniformity increases series resistance which reduces the productivity and stability of the device. The surface morphology of perovskite films has been significantly improved using a variety of techniques, including solvent vapor annealing [15–16], gas-blowing [17], amino halide additives [18-20], anti-solvent treatment [21, 22] and vacuum treatment [23]. Among these methods, the application of antisolvents during the creation of perovskite films proved to be quite remarkable in obtaining a pinhole-free and homogenous layer, which significantly enhanced the device's efficiency. Also, these anti-solvents accelerate perovskite nucleation, resulting in a homogeneous, pinhole-free film [24].

During the antisolvent engineering method, the physicochemical properties of solvents can lead to some complicated interactions. Some researchers used 12 antisolvents on perovskite solar cells. In this set, some were capable to tear down the perovskite film. Another group of researchers evaluated the dropping time effect of three different antisolvents on film formation [25]. Various research found that chlorobenzene, diethyl ether, and toluene are the best antisolvents for film formation [26-28] are the best antisolvents to produce a high-quality film in perovskite solar cells.

In this research, five different antisolvents namely, Diethyl ether (DE), Chloroform(CF), O-Dichlorobenzene (ODB), Chlorobenzene (CB), and Toluene (T) are used for the fabrication of mPSCs and also examine the impact of various antisolvents on film morphology and solar cell device performance.

2. Experimental Section

2.1 Materials and Method

Solaronix SA (Aubonee, Switzerland) produced printed monolithic carbon electrodes with multilayers (glass/FTO/c-TiO_2/mp-TiO_2/mp-ZrO_2/mp-carbon), which were heated at 400°C for 30 minutes before manufacturing and then allowed to cool to ambient temperature. A solution of pre-mixed organometal halide perovskite precursors; $MAPbI_3$ (containing lead iodide, methylammonium iodide, and 5-aminnovaleric acid hydroiodide in ϒ-butyrolactone) was bought from solaronix SA (Aubonee, Switzerland). Using an electronic digital micropipette, 0.5 µl of the perovskite precursor solution was injected through the monolithic carbon electrodes. After drop-casting, the produced films were spin-coated with 110 µl of each of five different anti-solvents (chlorobenzene, chloroform, diethyl ether, o-dichlorobenzene, and toluene) and then annealed at 100°C for 30 minutes. The fabricated mPSCs devices were then enclosed in ossila's E132 encapsulating epoxy.

2.2 Characterization

The characterization studies are carried out to assess the structural properties and surface morphology of fabricated mPSCs. Also, the electrical measurement performed to assess the photovoltaic performance of the fabricated device. An X-ray diffractometer was used to assess the structural properties (XRD, Model No; EMPYREAN) and surface morphology conducted using a scanning electron microscope (SEM, Model No; JEOL 7600).

The current density-voltage (J-V) properties measured using the Abet sunshine solar simulator (Model No. Oriel 3A), which simulates sunlight with an illumination intensity of 100 mW/cm^2. To assess the photovoltaic performance of the device, the active area of the cell was accurately controlled using a 0.16 cm^2 black metal mask.

3. Results and Discussion

The X-ray diffraction pattern in figure 1(a). Depicts the effects of A.S.T on the fabricated MScs (glass/FTO/mp-TiO_2/mp-ZrO_2/$MAPbI_3$/mp-carbon) films with various ant solvents. The signals at 14.0°, 28.4°, 31.8°, 40.5°, and 43.1° are the attribute peaks of the $MAPbI_3$ perovskite layer, the correlating planes are (110), (004), (310), (224) and (314). In all samples, the sharp diffraction peaks are detected at (2θ =26.3°) which signifies the (002) plane carbon. On the other hand, Figure.1(b) shows the introduction of ant solvent treatment greatly increases the diffraction peaks intensity (2θ =14.0 °(110) and 2θ = 28.4 (004)), the perovskite film with Tol as an ant solvent show better outperforms as compared to pure perovskite film and other (DE, CF, ODB, and CB) ant solvents.

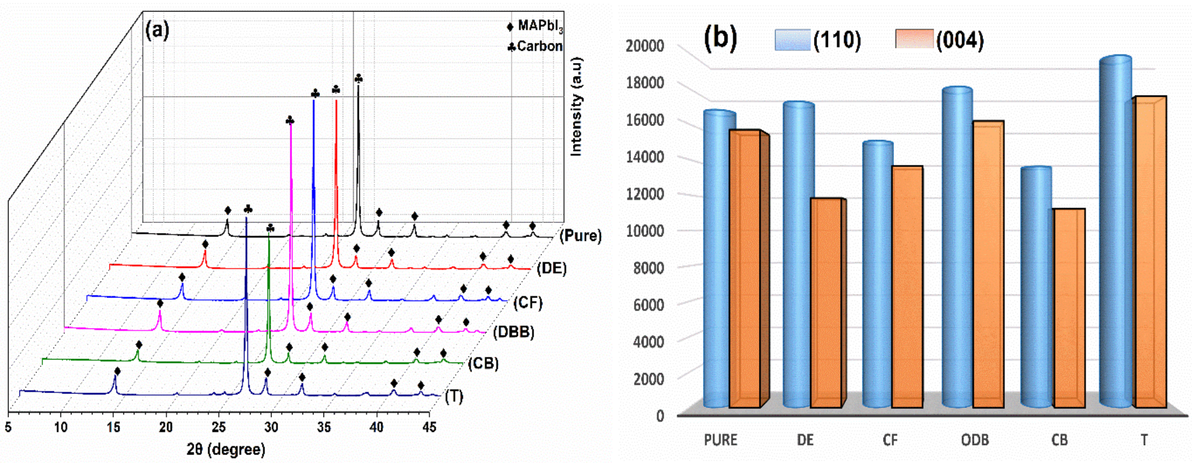

Figure 1: (a) XRD pattern of mPSCs films processed with different antisolvents, (b) a comparison of the (110) and (004) diffraction peaks' intensities under various antisolvent treatments.

The crystallization reached the highest when Tol was an antisolvent, which is indicating that the addition of A.S.T with moderate content changes the surface wettability and enhances the crystallization of perovskite film, which is reliable with the SEM result.

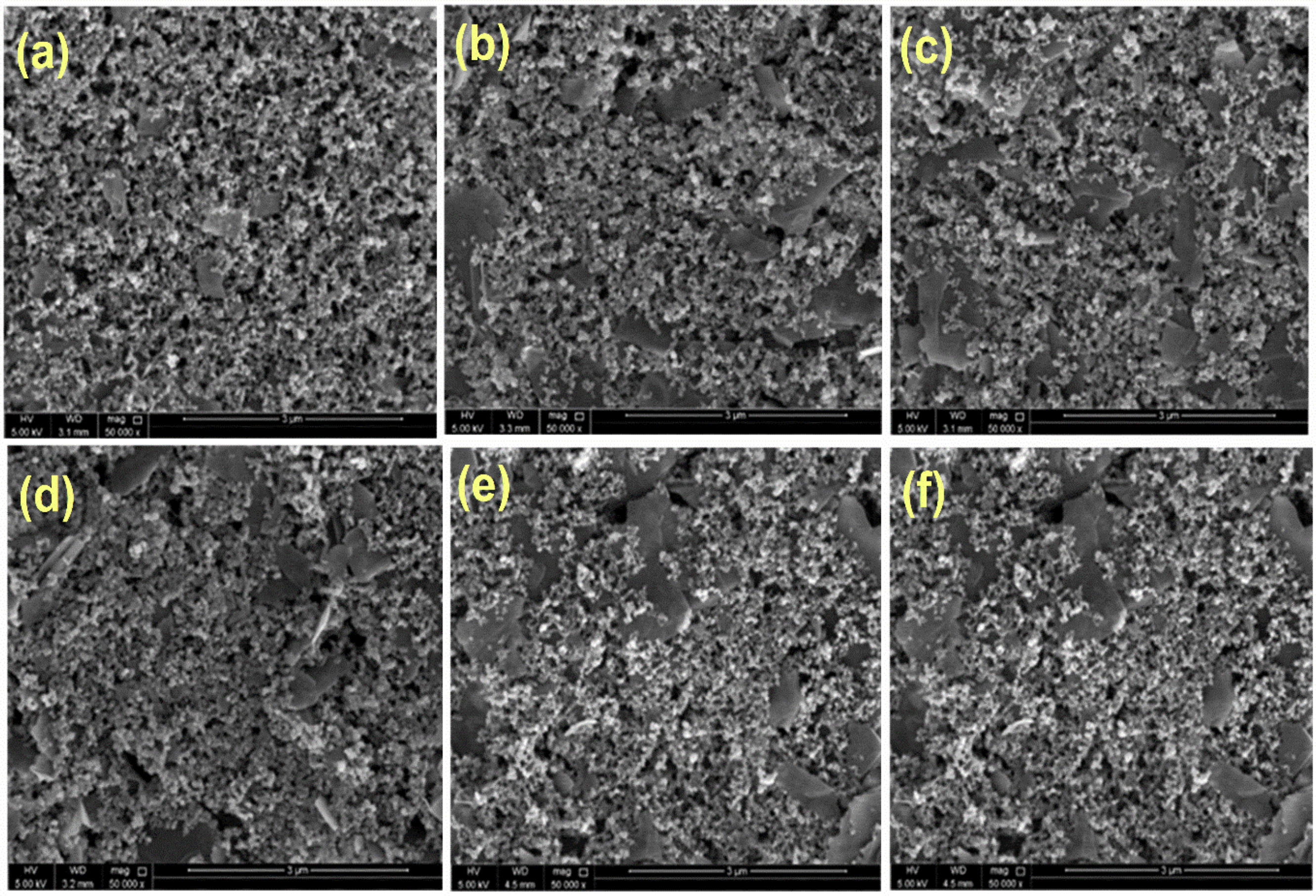

Figure 2. SEM images of mPSCs film in top view with various antisolvents.

The film is made up of only pure mPSCs exhibits (figure 2(a)) shows a rough surface, inadequate surface coverage, and several significant pinholes and cracks. In the case of anti-solvents (figure 2(b-e)), shows flakes-like structures develop on the surface of perovskite layers. As a result, when Tol an anti-solvent was applied to the perovskite film, only flake structures at the grain boundary were exposed. This is consistent with the XRD results and results in mechanical stress in the perovskite crystals, causing the major peaks ((110) and (004)) to be intensity increased. This perovskite with Tol antisolvent film, which resembles a layered, may have adequate surface area to expose more light-active sites, leading to high photovoltaic performance.

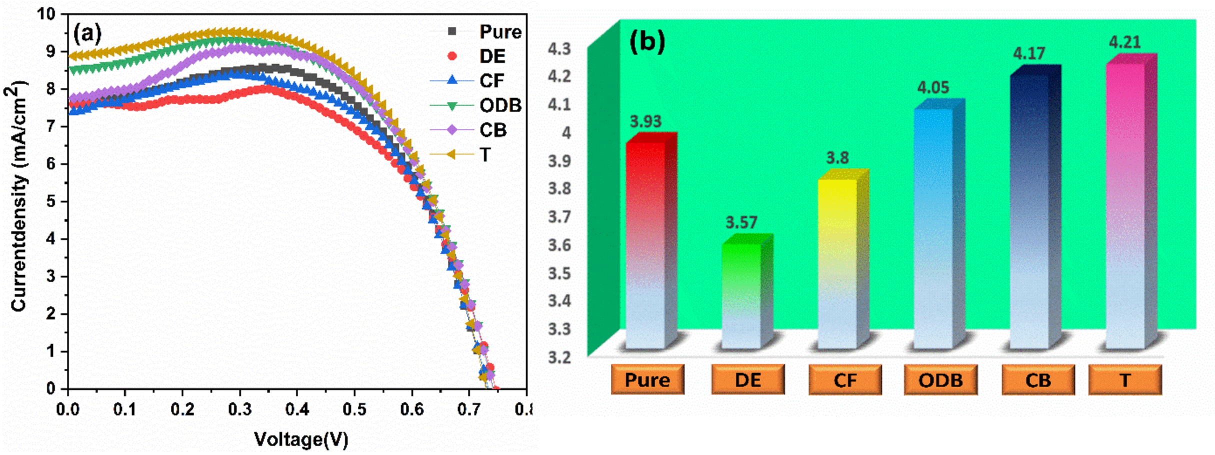

Figure 3: (a) J-V Cures and (b) statistic parameters of mPSCs film with different antisolvents.

Device	Voc, [V]	Jsc, [mA/cm^2]	FF, [%]	PCE, [%]
Pure	0.73	8.50	63.4	3.93
DE	0.75	7.53	63.2	3.57
CF	0.73	7.55	68.9	3.80
ODB	0.74	8.49	64.5	4.05
CB	0.74	8.93	74.8	4.17
T	0.72	8.94	65.4	4.21

Table 1: Photovoltaic parameter of mPSCs film with different ant solvents.

To determine the effects of applying different anti-solvents on the photo voltaic parameters such as short circuit current density (Jsc), open-circuit voltage (Voc), fill factor (FF), and PCE of the mPSC device. The current density-voltage (J-V) cures and statistic parameters of mPSCs device produced with various anti-solvents are shown in figure 3(a and b). The statistic parameters exhibit good consistency with good results, confirming the A.S.T. on fabricated mPSCs devices. The corresponding photovoltaic characteristics are presented in Table 1. The pure mPSCs device shows a PCE of 3.93%, with a V_{oc} of 0.73 V, J_{sc} of 8.50 mA/cm^2, and an FF of 63.4%. In the mPSCs device, DE and CF were used as antisolvents, and the PCE (3.57% and 3.80%) showed poor as compared to the pure mPSCs device. But in the A.S.T situation, in the case of ODB, CB, and Tol the PCE slightly increased. From all the above anti-solvents the Tol device shows the best PCE of 4.21%, with a V_{oc} of 0.72 V, a J_{sc} of 8.93 mA/cm^2, and FF of 75.4%, among all anti-solvents.

The enhancement in J_{sc}, V_{oc}, and FF, which results from better morphology and more crystallinity following A.S.T in Tol mPSCs device, account for the majority of the increase in PCE.

But in the case of pure mPSCs film have a rough surface and pinholes would decrease the PCE. Furthermore, anti-solvent treatment, which enhances higher crystallinity with smaller grain boundaries results in reduced charge traps, which help charge transfer even more. From all of the mPSCs devices, the Tol anti-solvent with device shows the best morphology and crystallinity, it obtains a good PCE.

Conclusion:

In summary, ant solvent solvent treatment has been successfully applied to monolithic perovskite solar cells (mPSCs). In this study, five different organic solvents (DE, CF, ODB, CB, and T) are used as antisolvents and their effect on the mPSCs. Due to enhanced perovskite film morphology and greater crystallinity, the antisolvent treatment results in a better PCE than the pure mPSCs device. Toluene performs the best among the five antisolvents (DE, CF, ODB, and CB) in terms of enhancing the effectiveness of mPSCs devices.

Acknowledgement

Authors thanks to the Department of Electronics & Communications Engineering (ECE), Himalayan University, Itanagar, Arunachal Pradesh, India, for their support to carry out this research work. Also, thanks to collaborative organizations VNR VJIET, Hyderabad, Telangana, India and MITS, Madanapalli, AP, India for their encouragement to accomplish the work successfully.

References

[1] Grätzel M The light, and shade of perovskite solar cells, Nat. Mater. 13 (2014) 838–842.

[2] Park N.-G. Organometal perovskite light absorbers toward a 20% efficiency low-cost solid-state mesoscopic solar cell, J. Phys. Chem. Lett 2013 4 2423–2429.

[3] Cai Y, Liang L, Gao P, Promise of commercialization: carbon materials for low-cost perovskite solar cells, Chin. Phys. B. 2018 27 018805.

[4] Liu Z, Sun B, Liu X, Han J, Ye H, Shi T, Tang Z, Liao G, Efficient carbon-based $CsPbBr_3$ inorganic perovskite solar cells by using Cu-phthalocyanine as the hole transport material, Nano-Micro Lett. 2018 10 2-13.

[5] Jiang P, Jones T.W, Duffy N.W, Anderson K.F, Bennett R, Grigore M, Marvig P, Xiong Y, Liu T, Sheng Y, Hong L, Hou X, Duan M, Hu Y, Rong Y, Wilson G.J, Han H, fully printable perovskite solar cells with highly conductive, low temperature, perovskite-compatible carbon electrode, Carbon 2018 129 830–836.

[6] Gong J, Zhou Z, Sumathy K, Yang H, Qiao Q, Activated graphene nanoplatelets as a counter electrode for dye-sensitized solar cells, J. Appl. Phys 2016 119 13550-1-13550-6.

[7] Back H, Kim J, Kim G, Kyun Kim T, Kang H, Kong J, Ho Lee S, Lee K., Interfacial modification of hole transport layers for efficient large-area perovskite solar cells achieved via blade-coating, Sol. Energy Mater. Sol. Cells 2016 144 309-315.

[8] Park M, Cho W, Lee G, Hong S. C, Kim M, Yoon J, Ahn N, Choi M , Highly Reproducible Large-Area Perovskite Solar Cell Fabrication via Continuous Megasonic Spray Coating of $CH_3NH_3PbI_3$ 2019 15 1804005.

[9] Di Giacomo F, Shanmugam S, Fledderus H, Bruijnaers B. J, Verhees W. J. H, Dorenkamper M. S, Veenstra S. C, Qiu W, Gehlhaar R, Merckx T., Aernouts T, Andriessen R, Galagan Y, Up-scalable sheet-to-sheet production of high efficiency perovskite module and solar cells on 6-in. substrate using slot die coating, Sol. Energy Mater. Sol. Cells 2018 181 53-59.

[10] Chang N. L, Ho-Baillie A. W. Y, Vak D, Gao M, Green M. A, Egan R. J, Manufacturing cost and market potential analysis of demonstrated roll-to-roll perovskite photovoltaic cell processes Sol. Energy Mater. Sol. Cells 2018 174 314.

[11] Matteucci F, Cina L, Lamanna E, Cacovich S, Divitini G, Midgley P. A, Ducati C, Di Carlo A, Encapsulation for long-term stability enhancement of perovskite solar cells 2016 30 62-172.

[12] Weerasinghe H. C, Dkhissi Y, Scully A. D, Caruso R. A, Cheng Y. B, Encapsulation for improving the lifetime of flexible perovskite solar cells, Nano Energy 2015 18 118-125.

[13] Wang D, Wright M, Elumalai N. K, Uddin A , Stability of perovskite solar cells, Sol. Energy Mater. Sol. Cells 2016 147 255-275.

[14] Asghar M. I, Zhang J, Wang H, Lund P. D, Renewable Sustainable Energy Rev 2017 77 131-146.

[15] Xiao Z, Dong Q, Bi C, Shao Y, Yuan Y, Huang J, Solvent Annealing of Perovskite-Induced Crystal Growth for Photovoltaic Device Efficiency Enhancement. Adv. Mater 2014 26 6503-6509.

[16] Lee Y. H, Luo J, Humphry-Baker R, Gao P, Gratzel M , Nazeeruddin M.K, Unraveling the Reasons for Efficiency Loss in Perovskite Solar Cells. Adv. Funct. Mater 2015 25 3925-3933.

[17] Huang F, Dkhissi Y, Huang W, Xiao M, Benesperi I, Rubanov S, Zhu Y, Lin X, Jiang L, Zhou Y, et al. Gas-Assisted Preparation of Lead Iodide Perovskite Films Consisting of a Monolayer of Single Crystalline Grains for High Efficiency Planar Solar Cells. Nano Energy 2014 10 10-18.

[18] Zhao Y, Zhu K, CH_3NH_3Cl-Assisted One-Step Solution Growth of $CH_3NH_3PbI_3$: Structure, Charge-Carrier Dynamics, and Photovoltaic Properties of Perovskite Solar Cells. J. Phys. Chem. C 2014 118 9412-9418.

[19] Zuo C, Ding L, An 80.11% FF Record Achieved for Perovskite Solar Cells by Using the NH_4Cl Additive. Nanoscale 2014 6 99359938.

[20] Bi D, Gao P, Scopelliti R, Oveisi E, Luo J, Gratzel M, Hagfeldt A, Nazeeruddin M. K, High-Performance Perovskite Solar Cells with Enhanced Environmental Stability Based on Amphiphile Modified $CH_3NH_3PbI_3$. Adv. Mater 2016 28 2910-2915.

[21] Xiao M, Huang F, Huang W, Dkhissi Y, Zhu Y, Etheridge J, Gray-Weale A, Bach U, Cheng Y.B, Spiccia L. A, Fast Deposition-Crystallization Procedure for Highly Efficient Lead Iodide Perovskite Thin-Film Solar Cells. Angew. Chem., Int. Ed 2014 53 9898-9903.

[22] Jeon N. J, Noh J.H, Kim Y.C, Yang W.S, Ryu S, Seok S. Il, Solvent Engineering for High-Performance Inorganic-organic Hybrid Perovskite Solar Cells. Nat. Mater 2014 13 897-903.

[23] Xie F.X, Zhang D, Su H, Ren X, Wong K.S, Gratzel M, Choy W.C.H, Vacuum-Assisted Thermal Annealing of $CH_3NH_3PbI_3$ for Highly Stable and Efficient Perovskite Solar Cells. ACS Nano 2015 9 639-646.

[24] Xiao M, Huang F, Huang W, Dkhissi Y, Zhu Y, Etheridge J, Gray-Weale A, Bach U, Cheng Y. B, Spiccia L, A fast deposition-crystallization procedure for highly efficient lead iodide perovskite thin-film solar cells, Angew. Chem., Int. Ed 2014 53 9898- 9903.

[25] Zheng X, Chen B, Wu C, Priya S, Room-Temperature Fabrication of $CH_3NH_3PbBr_3$ by Anti-Solvent Assisted Crystallization Approach for Perovskite Solar Cells with Fast Response and Small J−V Hysteresis. Nano Energy 2015 17 269−278.

[26] Jeon N.J, Noh J.H, Yang W.S, Kim Y.C, Ryu S, Seo J, Seok S. Il, Compositional Engineering of Perovskite Materials for High-Performance Solar Cells. Nature 2015 517 476−480.

[27] Bi D, Tress W, Dar M.I, Gao P, Luo J, Renevier C, Schenk K, Abate A, Giordano F, Correa Baena J-P, et al. Efficient Luminescent Solar Cells Based on Tailored Mixed-Cation Perovskites. Sci. Adv 2016 2 e1501170−e1501170.

[28] Son D-Y, Lee J-W, Choi Y.J, Jang Y. I-H, Lee S, Yoo P.J, Shin H, Ahn N, Choi M, Kim D, et al. Self-Formed Grain Boundary Healing Layer for Highly Efficient CH_3 NH_3PbI_3 Perovskite Solar Cells. Nat. Energy 2016 1 16081−16088.